LIMNOLOGY and OCEANOGRAPHY

ASLO

*Limnol. Oceanogr.* 66, 2021, 214–225

doi: 10.1002/lno.11598

# Dissolved organic carbon sorption dynamics in tidal marsh soils

**Andrew J. Pinsonneault [1]*, Patrick J. Neale [1], Maria Tzortziou [2], Elizabeth A. Canuel [3], Christina R. Pondell [3], Hannah Morrissette [4], Jonathan S. Lefcheck [1], James Patrick Megonigal [1]**

[1]Smithsonian Environmental Research Center, Edgewater, Maryland
[2]Department of Earth and Atmospheric Science, City College of New York, New York, New York
[3]Virginia Institute of Marine Science, William & Mary, Gloucester Point, Virginia
[4]University of Maryland Center for Environmental Science, Cambridge, Maryland

## *Abstract*

Coastal wetlands are significant sources of dissolved organic carbon (DOC) to adjacent waters and, consequently, exert a strong influence on the quantity and quality of DOC exported to the coastal oceans. Our understanding of the factors that control the exchange of DOC at the tidal marsh-estuarine interface, however, remains limited. We hypothesize that tidal marsh soils act as a regulator and that their physical characteristics, such as organic carbon content and mineral phase composition, are key controls on DOC exchange between soil surfaces and both surface and interstitial waters. To test this hypothesis, we generated traditional Langmuir sorption isotherms using anaerobic batch incubations of four tidal wetland soils, representing a range of soil organic carbon content (1.77% ± 0.12% to 36.2% ± 2.2%) and salinity regimes (freshwater to mixoeuhaline), across four salinity treatments. Results suggest that the maximum soil sorption capacity and DOC binding affinity increase and decrease with greater salinity, respectively, though the enhancement of maximum soil sorption capacity is somewhat mitigated in soils richer in poorly crystalline iron minerals. Initial natively sorbed organic carbon showed a significant positive correlation with soil specific surface area and K showed a moderate yet significant positive correlation with poorly crystalline iron mineral content. Taken together, these results point to a strong mineralogical control on tidal marsh sorption dynamics and a complex physicochemical response of those dynamics to salinity in tidal marsh soils.

Tidal wetlands are hotspots of biogeochemical exchange and transformation as well as some of the most productive ecosystems on Earth with net primary productivity commonly exceeding 600 g C $m^{-2}$ $yr^{-1}$ in the temperate zone (Megonigal and Neubauer 2009). These ecosystems occur in geomorphic settings that promote the exchange of water, solutes, and particulates with adjacent estuaries (Megonigal and Neubauer 2009), and they serve as significant sources of dissolved organic carbon (DOC) to the coastal ocean (Childers et al. 2000). The export of total organic carbon (TOC), of which DOC is a part, from tidal wetlands to coastal waters of the eastern United States alone is 1.2–2.9 Tg-C $yr^{-1}$ (Herrmann et al. 2015), supporting vital ecological functions such as microbial respiration, UV adsorption, and nutrient flux (Marschner and Kalbitz 2003). Despite the importance of wetland DOC export to estuarine ecosystem metabolism, there is relatively little understood about the processes that regulate DOC exchange at the tidal-estuarine interface.

Previous tidal marsh studies have reported that both DOC concentration ([DOC]) and optical characteristics differ dramatically between flooding tide and ebbing tide, with the ebb tide exhibiting greater concentration, molecular weight, and aromaticity (Tzortziou et al. 2008). DOC optical characteristics are a sensitive indicator of chemical composition and have been used to monitor variation in DOC sources and sinks over tidal cycles (Clark et al. 2008; Tzortziou et al. 2008). Complex interactions between biological and physical processes regulate the contribution of carbon sources to the DOC in interstitial waters that is ultimately exported from tidal wetland soils and sediments (Bertilsson and Jones 2003). Perhaps the least explored of these processes is the influence of DOC sorption-desorption on soil surfaces, a process that regulates DOC dynamics in upland forests and nontidal wetlands (e.g., Qualls 2000; Grybos et al. 2009) but remains largely unquantified in tidal wetland soils.

The sorption capacity of soils and sediments is strongly related to the content of poorly crystalline iron and aluminum oxides (McKnight et al. 1992; Kaiser and Guggenberger 2000). Poorly crystalline oxide surfaces have a high affinity for DOC and trace metals due primarily to their high specific surface

*Correspondence: pinsonneaulta@si.edu

Additional Supporting Information may be found in the online version of this article.

[Correction added on 15 October 2020, after first online publication: the order of authors in the byline was updated.]

area (Kaiser and Guggenberger 2000; Lalonde et al. 2012; Shields et al. 2016). As a result, poorly crystalline iron and aluminum oxide content is strong predictor of DOC sorption in both freshwater and marine sediments (McKnight et al. 1992; Lalonde et al. 2012; Shields et al. 2016) and well-drained terrestrial soils (Guggenberger and Kaiser 2003; Kaiser and Guggenberger 2003; Kothawala et al. 2009). Studies of mineral-organic associations in wetlands number far fewer compared to those in terrestrial systems, but are known to play a significant role in the release of dissolved organic matter via reductive dissolution of manganese and Fe oxyhydroxides in nontidal wetlands (Grybos et al. 2009). Due to the compositional heterogeneity of DOC and the poorly defined solubilities and surface characteristics of poorly crystalline metal oxides, the DOC affinity for metal oxide surfaces varies greatly (McKnight et al. 1992). However, the unique sorption mechanisms that are expected to operate in tidal wetland ecosystems where salinity is variable and rapidly changing remains largely unexplored and poorly understood.

The salinity environment of coastal wetlands is changing with sea level rise, with myriad and complex effects on carbon biogeochemistry. Increasing salinity is associated with decreases in soil carbon content, decreased inorganic nitrogen removal, and enhanced generation of sulfides (Herbert et al. 2015). The resulting increased ionic strength can also block or displace ions from soil exchange sites (Seitzinger et al. 1991; Stumm and Morgan 2012), and alter thermodynamic activity coefficients, leading to the dissolution of soil minerals such as iron (Baldwin et al. 2006). Thus, any research into DOC sorption dynamics in tidal wetlands should account for variations in salinity.

The objective of our study was to ascertain the dominant regulators of DOC exchange across tidal marshes that vary in salinity regime (freshwater to mixoeuhaline) and soil organic carbon content (mineral-dominated soils to highly organic soils). Based on the high specific surface area and reactivity of poorly crystalline iron and aluminum soil minerals (e.g., McKnight et al. 1992; Kaiser and Guggenberger 2000), and the role of ionic strength in blocking and displacing ions from reactive exchange sites at the mineral soil surface (Seitzinger et al. 1991; Stumm and Morgan 2012), we hypothesized that the variability in the DOC sorption capacity would increase with mineral content and decrease with salinity. The results of this work will ultimately be used to inform the development of a novel coupled hydrodynamic-photo-biogeochemical coastal wetlands model, the Finite Volume Community Ocean Model-Integrated Compartment Model (FVCOM-ICM; Clark et al. 2018), for wetland-estuarine interfaces.

## Methods

### Soil samples

We tested our hypothesis by examining the relationship between tidal marsh sediment composition, salinity environment, and DOC concentration. Our study sites were selected based on salinity environment, soil organic carbon content, and the specific surface area of the soil mineral component. Soil cores, 0–40 cm, were collected using a gouge corer between 05 March 2018 and 15 March 2018 from four tidal marshes in Chesapeake Bay, U.S.A.: (1) Kirkpatrick Marsh in Edgewater, Maryland, U.S.A. (home of the Global Change Research Wetland, 36°53′N, 76°33′W), (2) Jug Bay Wetlands Sanctuary in Lothian, Maryland, U.S.A. (38°46′N, 76°42′W), (3) Taskinas Marsh in Williamsburg, Virginia, U.S.A. (37°25′N, 76°43′W), and (4) Wachapreague Marsh in Wachapreague, Virginia, U.S.A. (37°32′N, 75°41′W) (Fig. 1; Table 1). Surface vegetation was carefully cut away and the soil cores were manually cut into 5 cm segments for the top 10 cm of the core, and then into 10 cm segments for the remaining 30 cm of the core, before being individually bagged and transported back to the lab on ice where they were immediately frozen at −80°C. Two separate cores were taken from each wetland for bulk density determination and particle size analysis. These cores were treated as described above with the exception that they were stored at 4°C for no more than 24 h prior to sample processing.

Bulk density was determined as per Blake and Hartge (1986) in which preweighed soil core segments of known length and diameter were oven-dried at 105°C for 72 h and reweighed. Soil core segments for particle size analysis were treated based on a method modified from Zobeck (2004) where soils were air-dried for 2 weeks and passed through a 1 mm mesh test sieve. The frozen core segments were dried in a Labconco console freeze-dryer, passed through a 1 mm mesh test sieve, and combined into bulk samples by depth increment and site.

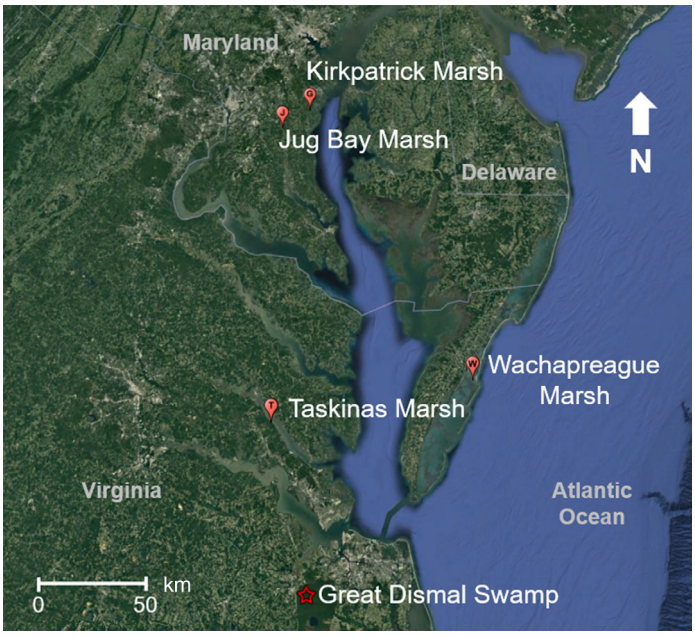


**Fig 1.** Composite satellite image from Google Earth displaying field site locations (Google Earth Pro V 7.3.2.5776, March 1, 2019).

**Table 1.** Tidal marsh surface characteristics and soil characteristics for 0–40 cm depth including SE.

| Characteristic | Kirkpatrick Marsh | Taskinas Marsh | Jug Bay Marsh | Wachapreague Marsh |
|---|---|---|---|---|
| Soil core GPS coordinates | 38°52′25.90″N 76°32′59.60″W | 37°24′48.79″N 76°42′57.44″W | 38°46′52.32″N 76°42′29.09″W | 37°35′56.33″N 75°38′9.38″W |
| Dominant vegetation at soil core collection site | *Schoenoplectus americanus* | *Spartina patens* | *Typha latifolia* | *Spartina alterniflora* |
| | *Spartina patens* | *Spartina alterniflora* | *Peltandra virginica* | *Salicornia europaea* |
| | *Distichlis spicata* | *Distichlis spicata* | *Nuphar lutea* | |
| Growing season surface-water salinity (psu) | 7.15 ± 0.55 | 14.8 ± 0 | $1.29 \times 10^{-1} \pm 4.50 \times 10^{-3}$ | 32.0 ± 0 |
| % Soil organic matter | 74.8 ± 0.2 | 39.3 ± 1.8 | 21.8 ± 0.6 | 5.12 ± 0.54 |
| % Total organic carbon | 36.2 ± 2.2 | 12.4 ± 0.3 | 7.29 ± 0.54 | 1.77 ± 0.12 |
| Bulk density (g $cm^{-3}$) | $1.08 \times 10^{-1} \pm 8.11 \times 10^{-3}$ | $1.71 \times 10^{-1} \pm 1.25 \times 10^{-2}$ | $3.05 \times 10^{-1} \pm 3.42 \times 10^{-2}$ | 1.99 ± 0.12 |
| Specific surface area ($m^2$ $g^{-1}$) | 10.5 ± 0.4 | 23.8 ± 1.7 | 40.8 ± 8.1 | 6.60 ± 1.09 |
| Poorly crystalline Al (mg $g^{-1}$) | $5.92 \times 10^{-1} \pm 3.02 \times 10^{-2}$ | 1.43 ± 0.08 | 1.22 ± 0.01 | $4.64 \times 10^{-1} \pm 1.33 \times 10^{-2}$ |
| Poorly crystalline Fe (mg $g^{-1}$) | $1.37 \times 10^{-1} \pm 3.54 \times 10^{-2}$ | 1.39 ± 0.46 | 11.2 ± 1.7 | 1.30 ± 0.28 |
| % Sand | 31.6 ± 9.8 | 46.2 ± 8.4 | 31.9 ± 6.6 | 40.6 ± 2.3 |
| % Silt | 60.4 ± 7.6 | 40.8 ± 6.1 | 57.0 ± 5.3 | 50.5 ± 2.3 |
| % Clay | 8.07 ± 2.4 | 13.0 ± 2.3 | 11.1 ± 1.3 | 8.95 ± 0.13 |
| Mean grain size ($\mu$m) | 39.8 ± 11.9 | 66.6 ± 30.6 | 35.2 ± 8.7 | 49.1 ± 3.2 |

Subsamples were taken from each freeze-dried depth increment bulk sample for percent soil organic matter, percent total organic carbon (%TOC), specific surface area, soil poorly crystalline iron, and soil poorly crystalline aluminum determination before the depth-increment bulk samples for each site were combined to form the four bulk soil samples (0–40 cm) used in the sorption incubation experiment. Processed soil samples were stored in desiccators for the duration of this study.

The soil organic matter fraction was determined in triplicate via loss on ignition at 450°C for 24 h using triplicate 2 g subsamples of freeze-dried soil (Heiri et al. 2001). Percent total organic carbon was determined following the methods described in Hedges and Stern (1984). Small subsamples (1–15 mg) of freeze-dried soil were fumigated overnight with 6 mol $L^{-1}$ HCl, dried, and packaged prior to analysis with a Carlo Erba Elemental Analyzer. Replicate analyses ($n$ = 2–4) were run for all samples and the analytical variability was less than 5%. Prior to analysis for specific surface area and particle size, dried soils (0.6–1.0 g) were combusted for 12 h at 350°C to remove organic material. Samples for specific area were degassed at 250°C for 2 h on a Micrometric Flow Prep 060 to remove water. Soils were then analyzed by nitrogen adsorption using a 5-point BET method with a Gemini V Surface Area Analyzer. Combusted samples analyzed for particle size were measured in triplicate with a Beckman Coulter LS 13320 Laser Diffraction Particle Size Analyzer. Determination of soil poorly crystalline aluminum and soil poorly crystalline iron content was based on methods described in Kostka and Luther (1994) where triplicate samples of 0.3 g of freeze-dried soil were treated with 30 mL of degassed 0.5 mol $L^{-1}$ HCl under anaerobic conditions, shaken on a horizontal shaker at 150 RPM for 1 h, and then centrifuged at 4700 × $g$ for 1 h. Twenty milliliters of the supernatant was treated with 200 $\mu$L of 6 mol $L^{-1}$ HCl and analyzed with an Agilent Technologies 7900 inductively coupled plasma mass spectrometer.

### Dissolved organic carbon

In April 2018, approximately 115 L of surface water was collected in acid-washed carboys from the Jericho Ditch (36°41′45.03″N, 76°30′28.16″W) in the Great Dismal Swamp National Wildlife Refuge, a nontidal forested wetland located on the coastal plain of southeastern Virginia and northeastern North Carolina, U.S.A. (36°37′N, 76°28′W; Fig. 1). The carboys were transported surrounded by bagged ice and covered with a thick tarp to prevent DOC photodegradation. Samples were stored at 4°C in the dark for no more than 24 h prior to sample processing.

The DOC in 115 L of Jericho ditch water was concentrated by reverse osmosis using a Growonix GX600 reverse osmosis system fitted with both pleated and spun sediment filters. The retentate was cycled back into the sample carboy, which was topped off with fresh sample as volume decreased, and the purified water was discarded except for a subsample that was

kept for DOC determination. The DOC concentrate was passed through a 20 $\mu$m pore size Whatman Polycap 75 HD disposable filter capsule followed by a 0.2 $\mu$m pore size Whatman Polycap 36 TC polyethersulfone membrane capsule before being stored at 4°C in the dark. The concentrate was then treated with enough sodium azide ($NaN_3$), a microbial inhibitor, to obtain a final concentration of 1 mmol $L^{-1}$ $NaN_3$. DOC concentration ([DOC]) was measured on a Shimadzu TOC-L using high-temperature combustion.

**Batch incubations**

The treated DOC concentrate had a [DOC] of 217 mg-DOC $L^{-1}$, a pH of 4.40, a salinity of 0.08 mg $g^{-1}$, and a specific conductivity of 180 $\mu$S $cm^{-1}$. This stock was portioned off into four substocks and instant ocean aquarium salt was added to three of the stocks to produce salinities of 0 psu (no instant ocean added), 10 psu, 20 psu, and 35 psu. Each of these stocks were used to prepare 7 "isotherm standards" ranging in [DOC] from 0 to $\sim$ 200 mg $L^{-1}$ by dilution with a "zero" DOC solution (< 0.2 mg-DOC $L^{-1}$; hereafter referred to as the dilutant) of similar pH, salinity, and specific conductivity prepared with ultrapure water, instant ocean aquarium salt, 1 mmol $L^{-1}$ $NaN_3$, and dilute HCl. Isotherm standards were freshly prepared for each batch incubation.

The batch incubations were performed based on methods described by Kothawala et al. (2008) under a 95% nitrogen ($N_2$) and 5% hydrogen ($H_2$) atmosphere in a Coy Laboratory Products anaerobic chamber using solutions degassed with $N_2$. Thirty milliliters of isotherm standard was added to triplicate samples of 1 g soil in 50 mL centrifuge tubes, capped, wrapped in aluminum foil, and laid flat in a horizontal shaker for 24 h at room temperature ($\sim$ 22°C) at a speed of 70 RPM. The samples were then centrifuged at 4700 × $g$ for 1 h, the supernatant decanted, and both salinity (WTW Multi 340i probe) and pH (Thermo Orion 3 Star pH meter) measured before the supernatant was syringe-filtered using disposable 0.45 $\mu$m Millex filter cartridges. Potential DOC contribution from the filter cartridges was avoided by discarding the first few milliliters of the filtrate for each sample.

**Sorption isotherms**

The traditional Langmuir isotherm (Eq. 1) accounts for the desorption of native adsorbed organic carbon ($C_0$) and expresses a relationship between the quantity of DOC adsorbed ($\Delta[DOC]_{0-f}$) in mg-DOC $g^{-1}$, the final DOC concentration ($[DOC]_f$) in mg-DOC $L^{-1}$, the bulk DOC binding affinity ($K$) in L $g^{-1}$, and the maximum soil sorption capacity ($Q_{max}$) in mg-DOC $g^{-1}$ (Kothawala et al. 2008).

$$\Delta[DOC]_{0-f} = \frac{\left(Q_{max} * K * [DOC]_f\right)}{\left(1 + \left(K * [DOC]_f\right)\right)} - C_0 \quad (1)$$

The Langmuir isotherm parameters, maximum soil sorption capacity, initial exchangeable organic carbon, and DOC binding affinity, were derived by fitting the $\Delta[DOC]_{0-f}$ vs. $\Delta[DOC]_f$ data using nonlinear regression as per Eq. 1. Due to the almost linear fit of the isotherms for Taskinas and Kirkpatrick in the 35 psu salinity incubations, the maximum soil sorption capacity for these isotherms were anomalously large and had a very large standard error (SE), suggesting that a wide range of maximum soil sorption capacity values would be an appropriate fit for the regression line. Consequently, the relationship between maximum soil sorption capacity and salinity for both Kirkpatrick and Taskinas soils was assumed to be linear and the maximum soil sorption capacity values derived for the 0, 10, and 20 psu salinity treatments were used to extrapolate the maximum soil sorption capacity values at 35 psu using the TREND function in Microsoft Excel. The TREND function calculates a linear trend given a series of dependent ($y$) and independent ($x$) variables and returns values along that trend line. Though the extrapolated maximum soil sorption capacity values reported fell within the range predicted by the non-linear regression, these two values were omitted from statistical analysis.

The null point (NP) is defined as the equilibrium concentration at which there is no net removal (adsorption) or release (desorption) of DOC from solution, the biogeochemical significance of which is a sorptive equilibrium between the soil mineral surfaces and the aqueous phase. The x-intercept of the fitted isotherm curves (Vandenbruwane et al. 2007) was calculated for each isotherm as the $[DOC]_f$ where $\Delta[DOC]_{0-f}$ = 0 mg-DOC $g^{-1}$ as per Eq. 2.

$$NP = \frac{C_0}{((Q_{max} - C_0) * K)} \quad (2)$$

Any statistics involving the null point omitted values for the 35 psu salinity treatment of the Kirkpatrick and Taskinas sites.

**Statistics**

Statistics were conducted using SigmaPlot 12.3, JMP 14.0, and RStudio 1.2.5033. Normality of the data set, or residuals in the case of multiple regression, was tested using the Shapiro-Wilk test, and homoscedasticity was determined using Levene's test. In the case of normality and equal variance, ANOVA with post hoc Tukey Honest Significant Difference test (Tukey HSD) was used to test for differences in group means. Stepwise regression was used to identify soil composition predictors for soil-specific surface area, multiple linear regression analysis was used to test the significance of the relationship, and studentized residuals were used to identify regression outliers. Linear mixed effect models (Supporting Information Table S1) were used to determine the relationship between maximum soil sorption capacity, salinity, and soil

poorly crystalline iron content and between DOC binding affinity and salinity with site as the random variable with the $r^2$ calculated using "piecewiseSEM" package in RStudio (Lefcheck 2016). In the case of unequal variance or when normality was not successfully obtained using log transformation, Kruskal–Wallis with post hoc Steel-Dwass was used to compare groups, Wilcoxon Ranked Sums to compare pairs, and Spearman correlations were used. Error estimates presented in this article are SE unless otherwise specified. Analyses were conducted on data derived from bulk soil samples unless otherwise specified.

## Results

### Soil characterization

The four locations in our study were selected to represent a wide range of characteristics expected to influence DOC sorption dynamics. The Kirkpatrick site had the highest soil organic matter and TOC content (75% and 35%, respectively) and consequently the lowest bulk density (0.11 g $cm^{-3}$) (Table 1). The Wachapreague site was lowest in soil organic matter and TOC (5% and 2%, respectively) and highest in bulk density (1.99 g $cm^{-3}$), and therefore had the most sand, silt, and clay of the four sites per volume (i.e., g $cm^{-3}$; Table 1). Except for the Wachapreague soil, the %TOC, percent soil organic matter, and bulk density reported here are comparable to the ranges of 3.1–48.3%, 5.80–87.9%, and 0.040–0.846 g $cm^{-3}$, respectively, reported by Williams and Rosenheim (2015) for freshwater and salt marshes and by Neubauer (2008) for tidal marsh soils along the Atlantic coast of the United States. Though the Wachapreague soil exhibited significantly higher bulk density than the other three marsh soils by a factor of $\sim 6.5$ due to its predominantly mineral makeup, the results were comparable to the soil bulk densities > 1.5 g $cm^{-3}$ previously measured at that site (L. Schile-Beers unpubl. data).

The variation in specific surface area, soil poorly crystalline iron content, and soil poorly crystalline aluminum content amongst our four tidal wetland soils highlights the wide range of mineralogy represented by these sites. These three mineralogical characteristics were independent of the percent mineral matter in the soil (i.e., 100% soil organic matter). Specific surface area and soil poorly crystalline iron content were greatest at the Jug Bay site, 41 $m^2$ $g^{-1}$ and 11 g $g^{-1}$, respectively, while

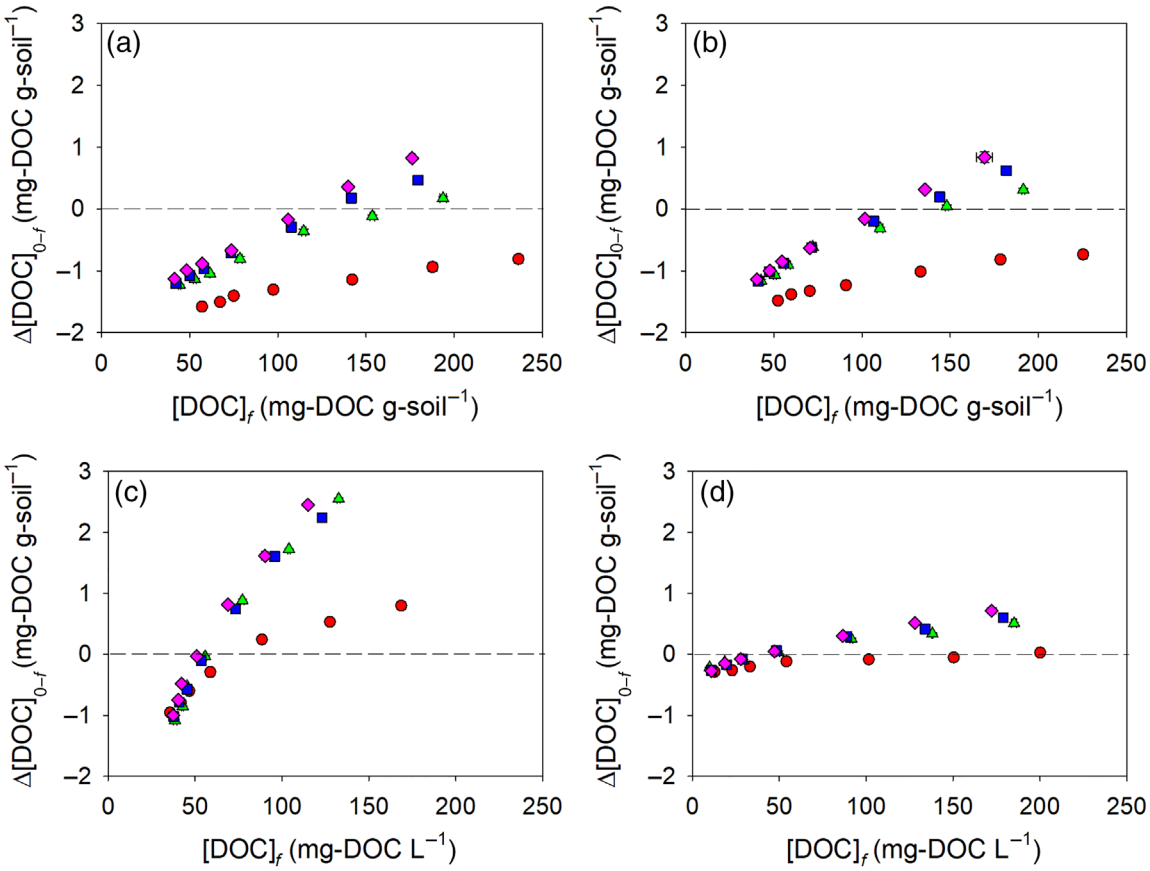


**Fig 2.** Traditional Langmuir isotherms across the four salinity treatments for (**a**) Kirkpatrick, (**b**) Taskinas, (**c**) Jug Bay, and (**d**) Wachapreague. Red circles, green triangles, blue squares, and purple diamonds reflect 0 psu, 10 psu, 20 psu, and 35 psu salinity treatments, respectively. Bidirectional error bars denote SE.

soil poorly crystalline aluminum content was greatest at the Taskinas site (1.5 mg $g^{-1}$). Specific surface area was lowest at the Wachapreague site (7 $m^2$ $g^{-1}$) while both soil poorly crystalline iron content and soil poorly crystalline aluminum content were lowest at the highly organic Kirkpatrick site (Table 1). This range of poorly crystalline mineral content fell within the range of $\sim$ 0.1–4.5 mg-Fe g-$soil^{-1}$ and $\sim$ 0.3–1.6 mg-Al g-$soil^{-1}$ reported by Marton and Roberts (2014) for Louisiana salt marsh soils with the exception of the Jug Bay soil which contained substantially greater soil poorly crystalline iron content. However, similar to our result of 11.2 ± 1.7 mg-Fe g-$soil^{-1}$, previous soil analyses conducted at Jug Bay by Keller et al. (2013) reported soil poorly crystalline iron content of $\sim$ 10 mg-Fe g-$soil^{-1}$ thereby validating our result. Specific surface area, soil poorly crystalline aluminum content, and soil poorly crystalline iron content all differed significantly among the four soils ($F_{3,10}$ = 45.4, $p < 0.001$, Tukey HSD ≤ 0.0431, $chi^2(3)$ = 47.6, $p < 0.0001$, and $chi^2(3)$ = 45.2, $p < 0.0001$, Steel-Dwass $p \leq 0.0004$) with the following exceptions: specific surface area did not differ significantly between Kirkpatrick and Wachapreague ($p$ = 0.055), soil poorly crystalline aluminum content did not differ significantly between Taskinas and Wachapreague soils ($p$ = 0.072), and soil poorly crystalline iron content did not differ significantly between Wachapreague and Taskinas soils ($p$ = 0.971). Multiple linear regression results suggested that soil poorly crystalline aluminum content and soil poorly crystalline iron content explained 84% of the variability in mineral specific surface area ($r^2_{adj}$ = 0.844, $F_{2,1}$ = 36.2, $p < 0.0001$, Std $\beta_{Al}$ = 0.440, Std $\beta_{Fe}$ = 0.703; Supporting Information Table S2).

The mineral phase particle size distribution of the Kirkpatrick, Jug Bay, and Wachapreague soils corresponded to that of a silty loam while that of the Taskinas soil corresponded to a loam (Liebens 2001), two soil textures commonly found in coastal wetlands (Lyu et al. 2015). Despite significant differences in mineralogy, the sand, silt, and clay fractions did not differ significantly among the four sites ($p$ = 0.15–0.47) nor were there any significant correlations between any of these particle size fractions and either specific surface area or poorly crystalline mineral content ($p > 0.342$, not shown). Mean % sand, %silt, and %clay differed by no more than 14%, 19%, and 5%, respectively, across all four sites (Table 1).

The initial pH of the four degassed Great Dismal Swamp DOC stocks used to prepare the isotherm standards was

**Table 2.** Mean and SE of sorption characteristics derived from the Langmuir isotherm by salinity treatment. $Q_{max}$, $C_0$, $K$, and NP refer to the soil maximum sorption capacity, initial exchangeable soil carbon, the DOC binding affinity, and the null point, respectively.

| Isotherm variable | Kirkpatrick | Taskinas | Jug Bay | Wachapreague |
|---|---|---|---|---|
| $Q_{max}$ (mg $g^{-1}$) | | | | |
| 0 psu | 2.28 ± 0.39 | 2.21 ± 0.24 | 5.85 ± 0.68 | $4.96 \times 10^{-1} \pm 4.12 \times 10^{-2}$ |
| 10 psu | 4.53 ± 0.45 | 4.14 ± 0.21 | 12.2 ± 0.4 | 1.61 ± 0.25 |
| 20 psu | 6.57 ± 1.03 | 7.23 ± 1.81 | 11.6 ± 0.3 | 1.73 ± 0.19 |
| 35 psu | 9.83 | 10.8 | 12.5 ± 0.7 | 2.72 ± 0.53 |
| $C_0$ (mg $g^{-1}$) | | | | |
| 0 psu | 2.11 ± 0.28 | 1.99 ± 0.18 | 4.20 ± 0.79 | $3.71 \times 10^{-1} \pm 4.79 \times 10^{-2}$ |
| 10 psu | 2.10 ± 0.15 | 2.26 ± 0.25 | 4.45 ± 0.42 | $2.88 \times 10^{-1} \pm 2.801 \times 10^{-2}$ |
| 20 psu | 2.06 ± 0.12 | 1.89 ± 0.14 | 4.44 ± 0.39 | $3.74 \times 10^{-1} \pm 3.59 \times 10^{-2}$ |
| 35 psu | 1.98 ± 0.04 | 1.93 ± 0.06 | 4.50 ± 0.59 | $3.50 \times 10^{-1} \pm 3.06 \times 10^{-2}$ |
| $K$ (L $g^{-1}$) | | | | |
| 0 psu | $5.55 \times 10^{-3} \pm 4.44 \times 10^{-3}$ | $6.06 \times 10^{-3} \pm 3.24 \times 10^{-3}$ | $3.45 \times 10^{-2} \pm 9.60 \times 10^{-3}$ | $1.55 \times 10^{-2} \pm 7.80 \times 10^{-3}$ |
| 10 psu | $5.17 \times 10^{-3} \pm 1.55 \times 10^{-3}$ | $8.44 \times 10^{-3} \pm 2.82 \times 10^{-3}$ | $1.01 \times 10^{-2} \pm 2.06 \times 10^{-3}$ | $5.04 \times 10^{-3} \pm 1.61 \times 10^{-3}$ |
| 20 psu | $3.52 \times 10^{-3} \pm 1.11 \times 10^{-3}$ | $2.88 \times 10^{-3} \pm 1.29 \times 10^{-3}$ | $1.12 \times 10^{-2} \pm 2.09 \times 10^{-3}$ | $6.84 \times 10^{-3} \pm 1.84 \times 10^{-3}$ |
| 35 psu | $2.21 \times 10^{-3} \pm 7.18 \times 10^{-5}$ | $1.97 \times 10^{-3} \pm 8.91 \times 10^{-5}$ | $1.08 \times 10^{-2} \pm 3.08 \times 10^{-3}$ | $3.69 \times 10^{-3} \pm 1.22 \times 10^{-3}$ |
| NP (mg $L^{-1}$) | | | | |
| 0 psu | 2250 | 1528 | 73.9 | 192 |
| 10 psu | 167 | 142 | 57.1 | 43.2 |
| 20 psu | 130 | 123 | 55.6 | 40.3 |
| 35 psu | 114 | 110 | 52.2 | 40.1 |
| $r^2$ | | | | |
| 0 psu | 0.912 | 0.958 | 0.991 | 0.889 |
| 10 psu | 0.988 | 0.982 | 0.995 | 0.975 |
| 20 psu | 0.991 | 0.985 | 0.996 | 0.978 |
| 35 psu | 0.991 | 0.980 | 0.992 | 0.982 |

4.60 ± 0.09. Postincubation pH increased significantly in all batch incubations with Kirkpatrick, Taskinas, Jug Bay, and Wachapreague yielding final pH values of 6.74 ± 0.03, 6.66 ± 0.04, 5.16 ± 0.05, and 6.94 ± 0.10, respectively, resulting in ΔpH of 1.96 ± 0.06, 1.87 ± 0.06, 0.37 ± 0.06, and 2.18 ± 0.10, respectively. pH change showed a significant negative correlation with soil poorly crystalline iron content (Spearman $p = -0.622$, $p < 0.0001$, not shown); however, Δsalinity did not exceed 2.5 psu in any of the soil incubations in this study. Incubations without soil were performed at 12.5 and 285 mg-DOC $L^{-1}$ across the four salinity treatments, but there were no significant differences in [DOC] between any of the pre- and postincubation pairings ($chi^2(1) = 4.76 \times 10^{-2}$ to 2.33, $p > 0.1$, Supporting Information Fig. S1), suggesting that there is no precipitation of DOC in the absence of soil in our experiments.

### Langmuir sorption isotherms

The sorption isotherm plots for all four marsh soils are presented in Fig. 2 and the sorption characteristics calculated using the traditional Langmuir isotherm approach are presented in Table 2. The lowest $r^2$ of the nonlinear regressions performed to fit the Langmuir isotherms for all soils across the four salinity treatments was 0.889 with a mean of 0.974 ± 0.007. For each individual soil, the maximum adsorption capacity maximum soil sorption capacity generally increased with salinity, the DOC binding affinity and null point tended to generally decrease with salinity, and native adsorbed organic carbon showed no consistent trend in response to salinity. The low specific surface area Wachapreague soils consistently yielded the lowest maximum soil sorption capacity, maximum soil sorption capacity, and initial exchangeable organic carbon across all salinity treatments with Maximum soil sorption capacity ranging between approximately 3 and 5 mg-C g-soil$^{-1}$ in the 0 psu and 35 psu salinity treatments, respectively, and a mean initial exchangeable organic carbon of $3.46 \times 10^{-1} \pm 3.45 \times 10^{-2}$ mg-C $g^{-1}$ (standard deviation [SD]). The high specific surface area, iron-rich Jug Bay soil, on the other hand, consistently yielded the greatest maximum soil sorption capacity and initial exchangeable organic carbon across all salinity treatments, with maximum soil sorption capacity ranging between approximately 6 and 13 mg-C g-soil$^{-1}$ in the 0 psu and 35 psu salinity treatments, respectively, and a mean initial exchangeable organic carbon of $4.40 \pm 1.15 \times 10^{-1}$ mg-C g-soil$^{-1}$ (SD).

The mineral Wachapreague soil incubations also yielded the lowest null point across all salinity treatments, ranging from 192 mg-DOC $L^{-1}$ to 40.1 mg-DOC $L^{-1}$ in the 0 psu and 35 psu salinity treatments, respectively, and the organic-rich Kirkpatrick soil incubations yielded the greatest null point, ranging from 2250 mg-DOC $L^{-1}$ to 114 mg-DOC $L^{-1}$ in the 0 psu and 35 psu salinity treatments, respectively (Table 2).

**Table 3.** Summary of a linear mixed effects model for sorption isotherm characteristics where $Q_{max}$ = soil maximum sorption capacity, $K$ = dissolved organic carbon binding affinity, [$Fe_{pc}$] = soil poorly crystalline iron content, AIC = Akaike information criterion, BIC = Bayesian information criterion, logLik = log likelihood. Full model summary statistics are presented in the Supporting Information.

**$Log_{10}(Q_{max})$**

**Marginal $r^2$ (fixed effects only) = 0.636; conditional $r^2$ (fixed + random effects) = 0.920**

**Random effects: Formula: ~1 | site**

| | (Intercept) | Residual |
|---|---|---|
| SD | $3.39 \times 10^{-1}$ | $1.12 \times 10^{-1}$ |

**Fixed effects: $log_{10}(Q_{max}) \sim$ Salinity * $Fe_{pc}$**

| | Value | SE | df | *t* value | *p* value |
|---|---|---|---|---|---|
| (Intercept) | $1.04 \times 10^{-1}$ | $2.26 \times 10^{-1}$ | 8 | $4.59 \times 10^{-1}$ | $6.58 \times 10^{-1}$ |
| Salinity (psu) | $2.36 \times 10^{-2}$ | $4.05 \times 10^{-3}$ | 8 | 5.82 | $4.00 \times 10^{-5}$ |
| [$Fe_{pc}$] (mg $g^{-1}$) | $6.68 \times 10^{-2}$ | $3.95 \times 10^{-2}$ | 2 | 1.69 | $2.33 \times 10^{-1}$ |
| Salinity : [$Fe_{pc}$] (psu : mg $g^{-1}$) | $-1.36 \times 10^{-3}$ | $5.80 \times 10^{-4}$ | 8 | −2.34 | $4.73 \times 10^{-2}$ |

**$Log_{10}(K)$**

**Marginal $r^2$ (fixed effects only) = 0.312; conditional $r^2$ (fixed + random effects) = 0.803**

**Random effects: Formula: ~1 | site**

| | (Intercept) | Residual |
|---|---|---|
| SD | $2.36 \times 10^{-1}$ | $1.49 \times 10^{-1}$ |

**Fixed effects: $log_{10}(K) \sim$ Salinity * $Fe_{pc}$**

| | Value | SE | df | *t* value | *p* value |
|---|---|---|---|---|---|
| (Intercept) | −1.96 | $1.34 \times 10^{-1}$ | 11 | −14.6 | 0 |
| Salinity (psu) | $-1.49 \times 10^{-2}$ | $3.07 \times 10^{-3}$ | 11 | −4.86 | $5.00 \times 10^{-4}$ |

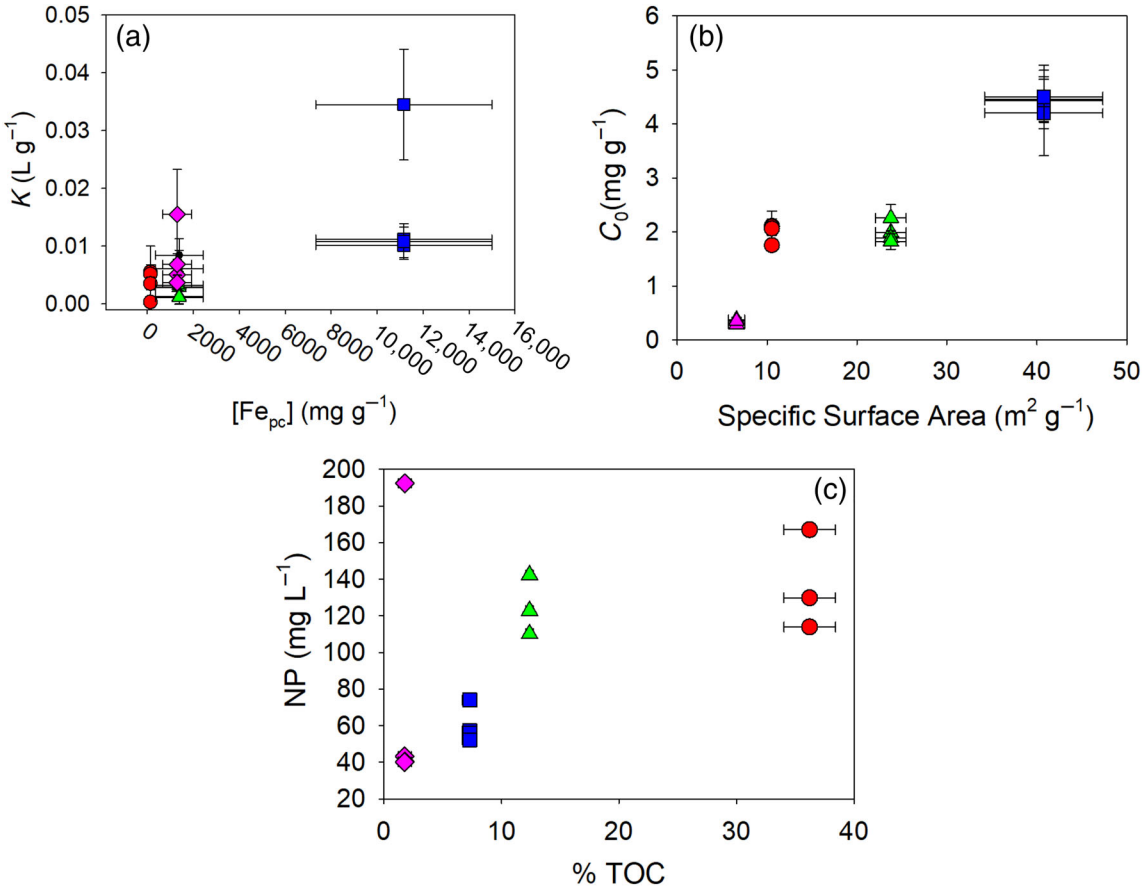


**Fig 3.** Scatterplot of (**a**) poorly crystalline iron ([$Fe_{pc}$]) vs. DOC binding affinity $K$ (Spearman $p = 0.546$, $p = 0.0288$, $n = 16$), (**b**) soil-specific surface area vs. natively sorbed DOC ($C_0$) (Spearman $p = 0.837$, $p < 0.0001$, $n = 16$), and (**c**) the percent total organic carbon (%TOC) vs. the null point (NP) (Spearman $p = -0.610$, $p = 0.0205$, $n = 14$). Red circles, green triangles, blue squares, and pink diamonds reflect Kirkpatrick, Taskinas, Jug Bay, and Wachapreague soils, respectively and error bars denote SE. Note that values for the Kirkpatrick and Taskinas null point at 0 psu were omitted from the correlation in graph (**c**).

Though $K$ tended to decrease with greater salinity for each individual soil, the soil with the greatest and least DOC binding affinity values did not remain consistent across the salinity treatments. The Jug Bay soil incubation yielded the highest $K$ in the 0 psu treatment and the Taskinas soil incubation yielded the lowest DOC binding affinity in the 35 psu salinity treatment with values of $1.08 \times 10^{-2} \pm 3.08 \times 10^{-3}$ L g$^{-1}$ and $3.45 \times 10^{-2} \pm 9.60 \times 10^{-3}$ L g$^{-1}$, respectively.

Linear mixed effect modeling results (Table 3) suggest that 64% of the variability in maximum soil sorption capacity can be explained by fixed effects only (salinity, soil poorly crystalline iron content, and the interaction between salinity and soil poorly crystalline iron content; $p \leq 0.0473$) though soil poorly crystalline iron content by itself was not a significant predictor ($p = 0.233$). This explained variability in maximum soil sorption capacity increased to 92% when both fixed and random (site) effects were included. Meanwhile, 80% of the variability in DOC binding affinity was explained by salinity alone with random effects (site) included (Table 3; $p = 0.0005$). Though soil poorly crystalline iron content was not a significant predictor for DOC binding affinity in the linear mixed effect model, the two correlated positively and significantly (Spearman $p = 0.546$, $p = 0.0288$; Fig. 3a). Similarly, initial exchangeable organic carbon correlated positively with specific surface area (Spearman $p = 0.837$, $p < 0.0001$; Fig. 3b) and the null point correlated positively with %TOC (Spearman $p = 0.667$, $p < 0.0001$, Fig. 3c).

## Discussion

Previous research on the sorption of solutes within soils has focused on terrestrial and nontidal wetland ecosystems; our study expands on this body of work by assessing the partitioning of DOC in disparate soils from four coastal tidal wetlands across a range of salinities and establishing relationships between sorption characteristics and key soil properties using traditional Langmuir isotherms. Our main finding suggests that, though both the maximum soil sorption capacity

(maximum soil sorption capacity) and DOC bonding affinity play key roles in sorption at the soil surface, changes in salinity influence the two differently with greater salinity increasing the soil sorption capacity but decreasing *K*. The enhancement of maximum soil sorption capacity with salinity was somewhat mitigated in wetland soils with greater poorly crystalline iron content though soil poorly crystalline iron content alone was not a significant predictor of maximum soil sorption capacity. These findings support our hypothesis that the variability in the quantity of DOC exchanged in tidal marsh soils is mainly a function of soil type and salinity and provide much-needed elucidation of the mechanisms of DOC exchange at the tidal marsh-estuarine interface.

**Soil texture**

The lack of significant difference in particle size distribution among our four wetland soils may be due to collecting our soil cores from high marsh locations ≥ 20 m from their respective tidal creek banks. Previous studies have reported that clays play a significant role in DOC sorption through their high surface area and charged surfaces (e.g., Guggenberger and Kaiser 2003). Suspended sediment particle size distribution tends to shift toward smaller, lighter particles such as clays with greater distance from the tidal creek as coarser, heavier sediments brought in with the flooding tide either settle out or are intercepted by surface vegetation (Moskalski and Sommerfield 2012). As such, it is possible that particle size plays a more significant role in DOC sorption in soils that are in closer proximity to a tidal creek. However, Moskalski and Sommerfield found that that the vast majority of suspended sediment concentration decrease occurred within ∼ 5 m of the tidal creek edge in a Delaware salt marsh. Consequently, as the marsh-area resolution in the FVCOM-ICM model is 10 m (Clark et al. 2018), larger than the near-creek area where the coarsest and heaviest particles are likely to settle or be intercepted, we do not expect the potential contribution of particle size relative to that of poorly crystalline hydrous Fe and Al oxides to affect our ability to apply our sorption results to model processes right at the wetland-tidal creek interface. However, future fieldwork and model development should certainly include more spatially heterogeneous sorption measurements to account for differences in sediment deposition.

**Sorption isotherms**

Kaiser and Guggenberger (2003) found that mineralogy controlled the relationship between specific surface area and the sorption of organic matter in forest soils. The significant, positive relationship between both soil poorly crystalline iron content and soil poorly crystalline aluminum content and specific surface area (Supporting Information Table S2), and a similar relationship between soil poorly crystalline iron content and the maximum soil sorption capacity (Table 3) suggest the DOC sorption in tidal marsh soils operates by similar mineralogical mechanisms. The significant positive correlations between DOC binding affinity and soil poorly crystalline iron content as well as between the quantity of initial soil exchangeable carbon and specific surface area also suggest that soils richer in poorly crystalline minerals, and, thus, with greater specific surface area, hosted a greater pool of natively sorbed DOC. The correlation between soil poorly crystalline iron content, and the lack of correlation with soil poorly crystalline aluminum content, on DOC binding affinity might stem from binding competition between Al and Fe for humic substances (Tipping et al. 2002), a major component of wetland DOC (Tzortziou et al. 2008), as humic acid binding affinities have been reported to be six times greater for Fe relative to Al (Bhandari et al. 1999).

**Impact of salinity on sorption isotherms**

Differences in salinity had a substantial impact on both maximum soil sorption capacity and DOC binding affinity, though the respective impact on each is notably different. The increase in maximum soil sorption capacity with greater salinity observed in our four tidal marsh soils was likely due to the direct ionic displacement of natively sorbed DOC (Kalbitz et al. 2000). The decrease in DOC binding affinity with greater salinity may stem from ionic strength-induced changes to dissolved humic structural conformation, essentially the 3D shape of the humic compounds. At high ionic strength, the charge repulsion between adjacent hydroxyl and carbonyl groups is neutralized resulting in the humic substance adopting a coiled conformation or shape (Baalousha et al. 2006) which, at the mineral surface, could result in fewer available attachment points (Tipping and Cooke 1982). Consequently, our results suggest that, though rising salinity may increase the number of potential sorption sites on the soil surface, it may decrease the ability of complex DOC compounds such as humic acids to bind to those sites. At low solute concentrations, these salinity effects have similar magnitudes, but operate in opposing directions, on sorption, such that their net effect is minimal (cf. Fig. 2). At high solute concentrations, maximum soil sorption capacity has the dominant influence so that sorption increases with salinity. Therefore, the influence of increased salinity on sorption processes in tidal marsh soils, and ultimately tidal marsh carbon export to estuarine waters, will interact with salinity-induced changes in [DOC].

Unlike Kothawala et al. (2009), we did not find a relationship between the null point and a combination of TOC and poorly crystalline mineralogy but only a positive correlation between TOC and the null point. A multiple linear regression of the null point vs. soil poorly crystalline aluminum content and soil poorly crystalline iron content in our data yielded a similar $r^2$, 0.3, to the 0.33 reported by Kothawala et al. (2009), but our regression residuals did not meet statistical assumptions of normality and equal variance. This might be due to our comparatively small sample size where we only analyzed four distinct soils compared to the 52 soils analyzed by Kothawala et al. (2009). The correlation between TOC and the null point in our data, however, does support their findings

that the organic carbon content of the soil influences the balance between adsorption and desorption of DOC.

Though quantifying the contribution of organic-organic sorption relative to mineral-organic sorption was outside the scope of this study, it is likely that cation and water-bridging, as well as the aforementioned H-bonding and van der Waals forces (Bolan et al. 2011), are important mechanisms in very organic tidal march soils such as those found at Kirkpatrick ($\sim$ 75% soil organic matter), where the ratio of soil poorly crystalline aluminum content + soil poorly crystalline iron content : TOC was found to be an order of magnitude lower than the other three soils. Soil organic matter contains a variety of functional groups that vary in polarity, such as anionic hydroxyls, uncharged aromatic moieties, and cationic amino groups. Consequently, in addition to soil mineralogy, the variation in abundance of these groups, specific surface area, and the chemical composition of soil organic matter has the potential to significantly influence soil sorption characteristics (Johnston and Tombácz 2002) and needs further study.

Similar to the increase in pH reported by Kothawala et al. (2009) in their sorption incubations of soils from volcanic B soil horizons, we observed an increase in pH in all our incubations, most notably in the Kirkpatrick, Taskinas, and Wachapreague soils. This supports ligand exchange as the dominant sorption mechanism in our soils as hydroxyl groups, which are coordinated to metal ions like Al and Fe on the soil surface, are replaced by organic ligands to form a surface complex; the release of these hydroxyl groups result in an increase in solution pH (McKnight et al. 1992). The comparatively small change in solution pH in Jug Bay incubations relative to the other three soils suggests that Jug Bay soils are relatively low in base saturation, a condition that is consistent with the fresh, low alkalinity setting of this site, and the observation that it was the only site with a negative correlation between ΔpH and soil poorly crystalline iron content.

It is possible that there was some dissolution of soil iron minerals due to the low initial pH of our DOC isotherm standards ($\sim$ 4.6) and high salinity in some of our treatments. However, due to the use of $NaN_3$ and conducting our experiments under anaerobic conditions, any dissolution would be chemical and not biotic and $Fe^{3+}$ would be reduced to $Fe^{2+}$ to which DOC has a much lower affinity for complexation (Riedel et al. 2013). The contribution of dissolution to the overall DOC removal from solution is further minimized by all four soils undergoing identical treatment and being compared only to one another. Elucidating the relative contributions of both sorption and complexation/precipitation to organo-mineral interactions in tidal marsh soils warrants further research.

## Implications for modeling sea level rise

Solute exchange at the soil surface has been extensively studied in terrestrial and nontidal wetland ecosystems, and it is well established that there is transformation and exchange of DOC at the tidal-estuarine interface. However, there remains a dearth of knowledge on the behavior of DOC in tidal wetland soils, and on the influence of soils on the amount and composition of DOC exchanged at the soil surface. The lack of mechanistic knowledge on DOC interactions with soils limits our ability to model marsh-estuarine carbon exchange using estuarine or Earth System Models, and to forecast the impacts of sea level rise, or other extreme or compounding disturbances impacting marsh soil characteristics, on carbon cycles at the terrestrial-aquatic interface (U.S. DOE 2017). Our study demonstrates that salinity and poorly crystalline iron are important abiotic controls on sorption processes in tidal wetlands. These parameters are commonly resolved in spatial databases and observational data sets, suggesting that forecast models could be refined to account for interactions between soil surfaces and DOC.

Tidal brackish and salt marshes are routinely exposed to salinity regimes that range from mesohaline to mixoeuhaline, while tidal freshwater marshes are routinely exposed to waters of $< 0.5$ psu. Salinity is increasing in coastal wetlands experiencing rising sea levels (Wigley 2005), though patterns of salinity change are complex due to the influence of factors such as changes in precipitation in the watersheds of rivers (Smith et al. 2005) and freshwater withdrawal (Knowles 2002). Our findings that increases in salinity influence soils sorption capacity and DOC binding affinity in opposing ways suggests that tidal marshes may be exhibiting complex physicochemical responses to increased salinity, with the balance between carbon sequestration (sorption) and mobilization (desorption) depending on the [DOC]. Further research into these sorption controls at greater soil depths and with more spatial variation will be instrumental in improving our understanding of tidal wetland sorption dynamics, and our ability to predict their responses to anthropogenic disturbances and global climate change.

## References

Bhandari, S. A., D. Amarasiriwardena, and B. Xing. 1999. Application of high performance size exclusion chromatography (HPSEC) with detection by inductively coupled plasma-mass spectrometry (ICP-MS) for the study of metal complexation properties of soil derived humic acid molecular fractions, p. 203–222. *In* G. Davies and E. A. Ghabbour. Humic substances: Advanced methods, properties, and applications. Royal Society of Chemistry.

Baalousha, M., M. Motelica-Heino, and P. L. Coustumer. 2006. Conformation and size of humic substances: Effects of major cation concentration and type, pH, salinity, and residence time. Colloids Surf. A Physicochem. Eng. Asp. **272**: 48–55. doi:10.1016/j.colsurfa.2005.07.010

Baldwin, D. S., G. N. Rees, A. M. Mitchell, G. Watson, and J. Williams. 2006. The short-term effects of salinization on anaerobic nutrient cycling and microbial community

structure in sediment from a freshwater wetland. Wetlands **26**: 455–464. doi:10.1672/0277-5212(2006)26[455:tseoso]2.0.co;2

Bertilsson, S., and J. B. Jones. 2003. 1 - Supply of dissolved organic matter to aquatic ecosystems: Autochthonous sources, p. 3–24. *In* S. E. G. Findlay and R. L. Sinsabaugh [eds.], Aquatic ecosystems. Academic Press.

Blake, G. R., and K. H. Hartge. 1986. Bulk density, p. 363–375. *In* A. Klute [ed.], Methods of soil analysis: Part 1—physical and mineralogical methods. Soil Science Society of America, American Society of Agronomy.

Bolan, N. S., D. C. Adriano, A. Kunhikrishnan, T. James, R. McDowell, and N. Senesi. 2011. Chapter one - Dissolved organic matter: Biogeochemistry, dynamics, and environmental significance in soils, p. 1–75. *In* D. L. Sparks [ed.], Advances in agronomy, v. **110**. Academic Press.

Childers, D. L., J. W. Day Jr., and H. N. McKellar Jr. 2000. Twenty more years of marsh and estuarine flux studies: Revisiting Nixon (1980). *In* M. Weinstein and D. A. Kreeger [eds.], Concepts and controversies in tidal marsh ecology. Kluer Academic Publishing.

Clark, C. D., L. P. Litz, and S. B. Grant. 2008. Saltmarshes as a source of chromophoric dissolved organic matter (CDOM) to Southern California coastal waters. Limnol. Oceanogr. **53**: 1923–1933. doi:10.4319/lo.2008.53.5.1923

Clark, J. B., W. Long, M. Tzortziou, P. J. Neale, and R. R. Hood. 2018. Wind-driven dissolved organic matter dynamics in a Chesapeake Bay tidal marsh-estuary system. Estuaries Coast. **41**: 708–723. doi:10.1007/s12237-017-0295-1

Google Earth Pro V 7.3.2.5776. March 1, 2019. Chesapeake Bay, USA, 37°50′25.59" N, 76°09′25.01" W, Eye alt 442 m.

Grybos, M., M. Davranche, G. Gruau, P. Petitjean, and M. Pédrot. 2009. Increasing pH drives organic matter solubilization from wetland soils under reducing conditions. Geoderma **154**: 13–19. doi:10.1016/j.geoderma.2009.09.001

Guggenberger, G., and K. Kaiser. 2003. Dissolved organic matter in soil: Challenging the paradigm of sorptive preservation. Geoderma **113**: 293–310. doi:10.1016/s0016-7061(02)00366-x

Hedges, J. I., and J. H. Stern. 1984. Carbon and nitrogen determinations of carbonate-containing solids. Limnol. Oceanogr. **29**: 657–663. doi:10.4319/lo.1984.29.3.0657

Heiri, O., A. F. Lotter, and G. Lemcke. 2001. Loss on ignition as a method for estimating organic and carbonate content in sediments: Reproducibility and comparability of results. J. Paleolimnol. **25**: 101–110. doi:10.1023/a:1008119611481

Herbert, E. R., and others. 2015. A global perspective on wetland salinization: Ecological consequences of a growing threat to freshwater wetlands. Ecosphere **6**: art206. doi:10.1890/es14-00534.1

Herrmann, M., and others. 2015. Net ecosystem production and organic carbon balance of U.S. East Coast estuaries: A synthesis approach. Global Biogeochem. Cycles **29**: 96–111. doi:10.1002/2013gb004736

Johnston, C. T., and E. Tombácz. 2002. Surface chemistry of soil minerals, p. 37–67. *In* J. B. Dixon and D. G. Shulze Soil mineralogy with environmental applications. SSSA Book Series, Vol 7. Soil Science Society of America.

Kaiser, K., and G. Guggenberger. 2000. The role of DOM sorption to mineral surfaces in the preservation of organic matter in soils. Org. Geochem. **31**: 711–725. doi:10.1016/s0146-6380(00)00046-2

Kaiser, K., and G. Guggenberger. 2003. Mineral surfaces and soil organic matter. Eur. J. Soil Sci. **54**: 219–236. doi:10.1046/j.1365-2389.2003.00544.x

Kalbitz, K., S. Solinger, J. H. Park, B. Michalzik, and E. Matzner. 2000. Controls on the dynamics of dissolved organic matter in soils: A review. Soil Sci. **165**: 277–304. doi:10.1097/00010694-200004000-00001

Keller, J. K., A. E. Sutton-Grier, A. L. Bullock, and J. P. Megonigal. 2013. Anaerobic metabolism in tidal freshwater wetlands: I. Plant removal effects on iron reduction and methanogenesis. Estuaries Coast. **36**: 457–470. doi:10.1007/s12237-012-9527-6

Knowles, N. 2002. Natural and management influences on freshwater inflows and salinity in the San Francisco Estuary at monthly to interannual scales. Water Resour. Res. **38**: 1289. doi:10.1029/2001WR000360

Kostka, J. E., and G. W. Luther. 1994. Partitioning and speciation of solid phase iron in saltmarsh sediments. Geochim. Cosmochim. Acta **58**: 1701–1710. doi:10.1016/0016-7037(94)90531-2

Kothawala, D. N., T. R. Moore, and W. H. Hendershot. 2008. Adsorption of dissolved organic carbon to mineral soils: A comparison of four isotherm approaches. Geoderma **148**: 43–50. doi:10.1016/j.geoderma.2008.09.004

Kothawala, D. N., T. R. Moore, and W. H. Hendershot. 2009. Soil properties controlling the adsorption of dissolved organic carbon to mineral soils. Soil Sci. Soc. Am. J. **73**: 1831. doi:10.2136/sssaj2008.0254

Lalonde, K., A. Mucci, A. Ouellet, and Y. Gélinas. 2012. Preservation of organic matter in sediments promoted by iron. Nature **483**: 198–200. doi:10.1038/nature10855

Lefcheck, J. S. 2016. piecewiseSEM: Piecewise structural equation modelling in r for ecology, evolution, and systematics. Methods Ecol. Evol. **7**: 573–579. doi:10.1111/2041-210X.12512

Liebens, J. 2001. Spreadsheet macro to determine USDA soil textural subclasses. Commun. Soil Sci. Plant Anal. **32**: 255–265. doi:10.1081/CSS-100103005

Lyu, X., and others. 2015. Changes of soil particle size distribution in tidal flats in the Yellow River delta. PLoS One **10**: e0121368. doi:10.1371/journal.pone.0121368

Marschner, B., and K. Kalbitz. 2003. Controls of bioavailability and biodegradability of dissolved organic matter in soils. Geoderma **113**: 211–235. doi:10.1016/s0016-7061(02)00362-2

Marton, J. M., and B. J. Roberts. 2014. Spatial variability of phosphorus sorption dynamics in Louisiana salt marshes.

J. Geophys. Res. Biogeosci. **119**: 451–465. doi:10.1002/2013jg002486

McKnight, D. M., K. E. Bencala, G. W. Zellweger, G. R. Aiken, G. L. Feder, and K. A. Thorn. 1992. Sorption of dissolved organic carbon by hydrous aluminum and iron oxides occurring at the confluence of Deer Creek with the Snake River, Summit County, Colorado. Environ. Sci. Technol. **26**: 1388–1396. doi:10.1021/es00031a017

Megonigal, J. P., and S. C. Neubauer. 2009. Biogeochemistry of tidal freshwater wetlands, p. 535–562. *In* G. M. E. Perillo, E. Wolanski, D. R. Cahoon, and M. M. Brinson [eds.], Coastal wetlands: An integrated ecological approach. Elsevier.

Moskalski, S. M., and C. K. Sommerfield. 2012. Suspended sediment deposition and trapping efficiency in a Delaware salt marsh. Geomorphology **139–140**: 195–204. doi:10.1016/j.geomorph.2011.10.018

Neubauer, S. C. 2008. Contributions of mineral and organic components to tidal freshwater marsh accretion. Estuar. Coast. Shelf Sci. **78**: 78–88. doi:10.1016/j.ecss.2007.11.011

Qualls, R. G. 2000. Comparison of the behavior of soluble organic and inorganic nutrients in forest soils. For. Ecol. Manage. **138**: 29–50. doi:10.1016/s0378-1127(00)00410-2

Riedel, T., D. Zak, H. Biester, and T. Dittmar. 2013. Iron traps terrestrially derived dissolved organic matter at redox interfaces. Proc. Natl. Acad. Sci. USA **110**: 10101. doi:10.1073/pnas.1221487110

Seitzinger, S. P., W. S. Gardner, and A. K. Spratt. 1991. The effect of salinity on ammonium sorption in aquatic sediments: Implications for benthic nutrient recycling. Estuaries **14**: 167–174. doi:10.2307/1351690

Shields, M. R., T. S. Bianchi, Y. Gélinas, M. A. Allison, and R. R. Twilley. 2016. Enhanced terrestrial carbon preservation promoted by reactive iron in deltaic sediments. Geophys. Res. Lett. **43**: 1149–1157. doi:10.1002/2015gl067388

Smith, S. J., A. M. Thomson, N. J. Rosenberg, R. C. Izaurralde, R. A. Brown, and T. M. L. Wigley. 2005. Climate change impacts for the conterminous USA: An integrated assessment. Clim. Chang. **69**: 7–25. doi:10.1007/s10584-005-3614-7

Stumm, W., and J. J. Morgan. 2012. Aquatic chemistry: Chemical equilibria and rates in natural waters. 3, New York: Wiley.

Tipping, E., and D. Cooke. 1982. The effects of adsorbed humic substances on the surface charge of goethite (α-FeOOH) in freshwaters. Geochim. Cosmochim. Acta **46**: 75–80. doi:10.1016/0016-7037(82)90292-7

Tipping, E., C. Rey-Castro, S. E. Bryan, and J. Hamilton-Taylor. 2002. Al(III) and Fe(III) binding by humic substances in freshwaters, and implications for trace metal speciation. Geochim. Cosmochim. Acta **66**: 3211–3224. doi:10.1016/S0016-7037(02)00930-4

Tzortziou, M., P. J. Neale, C. L. Osburn, J. P. Megonigal, N. Maie, and R. Jaffé. 2008. Tidal marshes as a source of optically and chemically distinctive colored dissolved organic matter in the Chesapeake Bay. Limnol. Oceanogr. **53**: 148–159. doi:10.4319/lo.2008.53.1.0148

U.S. DOE. 2017. Research priorities to incorporate terrestrial-aquatic interfaces in earth system models: Workshop report. DOE/SC-0187. U.S. Department of Energy Office of Science.

Vandenbruwane, J., S. De Neve, R. G. Qualls, S. Sleutel, and G. Hofman. 2007. Comparison of different isotherm models for dissolved organic carbon (DOC) and nitrogen (DON) sorption to mineral soil. Geoderma **139**: 144–153. doi:10.1016/j.geoderma.2007.01.012

Wigley, T. M. L. 2005. The climate change commitment. Science **307**: 1766. doi:10.1126/science.1103934

Williams, E. K., and B. E. Rosenheim. 2015. What happens to soil organic carbon as coastal marsh ecosystems change in response to increasing salinity? An exploration using ramped pyrolysis: Fate of coastal SOC with salinity. Geochem. Geophys. Geosyst. **16**: 2322–2335. doi:10.1002/2015GC005839

Zobeck, T. M. 2004. Rapid soil particle size analyses using laser diffraction. Appl. Eng. Agric. **20**: 633–639. doi:10.13031/2013.17466

## Acknowledgments

We would like to thank the staff of the Jug Bay Wetlands Sanctuary, the York River State Park, the Virginia Institute of Marine Science (VIMS) Eastern Shore Laboratory, and the Great Dismal Swamp National Wildlife Refuge for their support and assistance. In particular, we are grateful to Amanda Knobloch, Yanhua Feng, and Sean Fate (VIMS), Willy Reay (Chesapeake Bay National Estuarine Research Reserve), Michael Gonsior (University of Maryland Center for Environmental Science, Chesapeake Biological Laboratory), Jade Dominique Walker (University of Maryland University College), Ellen Weber (Wilkes University), and Andrew Peresta (Smithsonian Environmental Research Center) for their assistance in the field and laboratory. This study was funded by National Science Foundation Grant DEB-1556556; NASA Grant NNX14AP06G; NSF-LTREB Program support of the Global Change Research Wetland (DEB-0950080, DEB-1457100, DEB-1557009); and the Smithsonian Environmental Research Center. This paper is Contribution No. 3932 of the Virginia Institute of Marine Science, William & Mary.

## Conflict of Interest

None declared.

*Submitted 07 August 2019*
*Revised 02 June 2020*
*Accepted 20 August 2020*

*Editor-in-Chief: K. David Hambright*